MmTX1 and MmTX2 from coral snake venom potently modulate $GABA_A$ receptor activity

Jean-Pierre Rosso[a,1], Jürgen R. Schwarz[b,1], Marcelo Diaz-Bustamante[c,1], Brigitte Céard[a], José M. Gutiérrez[d], Matthias Kneussel[b], Olaf Pongs[e], Frank Bosmans[f,g,2], and Pierre E. Bougis[a,2]

[a]Aix Marseille Université, CNRS, Centre de Recherche en Neurobiologie et Neurophysiologie de Marseille UMR7286, 13344 Marseille, France; [b]Institute of Molecular Neurogenetics, Zentrum für Molekulare Neurobiologie Hamburg, University Medical Center Hamburg-Eppendorf, 20251 Hamburg, Germany; [c]Lieber Institute for Brain Development, Johns Hopkins University School of Medicine, Baltimore, MD 21205; [d]Instituto Clodomiro Picado, Facultad de Microbiología, Universidad de Costa Rica, 11501 San Jose, Costa Rica; [e]Institut für Physiologie, Universität des Saarlandes, 66424 Homburg, Germany; and [f]Department of Physiology and [g]Solomon H. Snyder Department of Neuroscience, Johns Hopkins University School of Medicine, Baltimore, MD 21205

Edited by Bruce P. Bean, Harvard Medical School, Boston, MA, and approved January 12, 2015 (received for review August 12, 2014)

$GABA_A$ receptors shape synaptic transmission by modulating Cl^- conductance across the cell membrane. Remarkably, animal toxins that specifically target $GABA_A$ receptors have not been identified. Here, we report the discovery of micrurotoxin1 (MmTX1) and MmTX2, two toxins present in Costa Rican coral snake venom that tightly bind to $GABA_A$ receptors at subnanomolar concentrations. Studies with recombinant and synthetic toxin variants on hippocampal neurons and cells expressing common receptor compositions suggest that MmTX1 and MmTX2 allosterically increase $GABA_A$ receptor susceptibility to agonist, thereby potentiating receptor opening as well as desensitization, possibly by interacting with the α^+/β^- interface. Moreover, hippocampal neuron excitability measurements reveal toxin-induced transitory network inhibition, followed by an increase in spontaneous activity. In concert, toxin injections into mouse brain result in reduced basal activity between intense seizures. Altogether, we characterized two animal toxins that enhance $GABA_A$ receptor sensitivity to agonist, thereby establishing a previously unidentified class of tools to study this receptor family.

coral snake toxin | MmTX1 | MmTX2 | GABA(A) receptor | hippocampal neurons

Ionotropic γ-aminobutyric acid type A ($GABA_A$) receptors are found predominantly in the central nervous system, where they mediate inhibitory postsynaptic transmission by influencing Cl^- flux across the cell membrane (1–4). Imbalances between excitatory and inhibitory $GABA_A$ receptor activity have been implicated in clinical phenotypes such as epilepsy, schizophrenia, and chronic pain (5, 6). As such, $GABA_A$ receptors are targeted by various drugs including barbiturates, benzodiazepines, and anesthetics (1, 7).

$GABA_A$ receptors belong to the pentameric Cys-loop superfamily of ligand-gated ion channel receptors, which also encompasses the nicotinic acetylcholine (nAChRs), glycine (GlyR), and serotonin receptors (8). The numerous subunit isoforms (α1–6, β1–3, γ1–3, δ, ε, π, θ, and ρ1–3) that can make up a $GABA_A$ receptor create multiple structural arrangements (9–11). In general, each subunit consists of four transmembrane domains, in which transmembrane domain 2 delineates the axially positioned Cl^- channel (12). Molecules can interact with various regions within one or more subunits, resulting in a complex pharmacologic landscape. For example, GABA, as well as the prototypic exogenous agonist muscimol (13), binds at the extracellular interface between a β and α subunit (β^+/α^-) (14, 15) whereas benzodiazepines require both the α and γ2 subunit to be pharmacologically active (16, 17). Conversely, anesthetics such as propofol most likely position themselves in transmembrane intersubunit pockets (18). So far, picrotoxin (PTX) is the only well-documented naturally occurring plant toxin that is known to block the $GABA_A$ receptor pore and is experimentally used as a chemoconvulsant to induce epileptic seizures (19). In contrast, molecules isolated from plant extracts and snake and cone snail venoms have been used extensively to probe the structural and functional properties of nAChRs (20, 21).

Here, we explore whether animal venoms contain toxins that primarily interact with $GABA_A$ receptors. While examining the venom of Costa Rican coral snakes (22), we came across a major fraction that displayed evidence of $GABA_A$-related toxicity in mice. Within this fraction, we found micrurotoxin1 (MmTX1) and MmTX2, two equally potent peptides with a primary sequence belonging to the PATE-SLURP1-LYNX1-Ly-6/neurotoxin-like family (23–25). Extensive binding and competition studies revealed that $GABA_A$ receptors are the primary target of these peptides, whereas nAChRs are unaffected. In contrast to PTX, which blocks the pore at micromolar concentrations, our data suggest that MmTX1 and MmTX2 modulate $GABA_A$ receptor function at subnanomolar quantities by tightly binding to the α^+/β^- subunit interface, a novel benzodiazepine-like binding site with promising therapeutic potential (26). Electrophysiologic experiments with recombinantly and synthetically produced MmTX1 and MmTX2 on hippocampal neurons, HEK 293 cells, and *Xenopus* oocytes expressing common receptor compositions indicate that these toxins allosterically increase $GABA_A$ receptor sensitivity to agonist, thereby reshaping channel opening as well as desensitization. Overall, our results demonstrate that potent and selective $GABA_A$-receptor modulating toxins can be found in

Significance

In this study, we report the identification of the first potent $GABA_A$ receptor-targeting toxins, to our knowledge, in snake venom, which provides a conceptual example for discovering novel ligands to study this receptor family, both functionally and structurally. Moreover, successful synthetic and recombinant production of these toxins [micrurotoxin1 (MmTX1) and MmTX2] will be valuable to further enhance their subtype selectivity or potency. In a broader context, both toxins may provide tools to evoke seizures in assays geared toward testing antiepileptic drugs or as lead molecules for designing therapeutics that modulate $GABA_A$ receptor activity.

Author contributions: M.D.-B., O.P., F.B., and P.E.B. designed research; J.-P.R., J.R.S., M.D.-B., B.C., J.M.G., F.B., and P.E.B. performed research; J.-P.R., J.R.S., M.D.-B., B.C., J.M.G., M.K., O.P., F.B., and P.E.B. contributed new reagents/analytic tools; J.R.S., M.D.-B., M.K., O.P., F.B., and P.E.B. analyzed data; and J.-P.R., J.R.S., M.D.-B., J.M.G., M.K., O.P., F.B., and P.E.B. wrote the paper.

The authors declare no conflict of interest.

This article is a PNAS Direct Submission.

Data deposition: The protein sequence data reported in this paper have been deposited in the UniProt Knowledgebase [accession nos. C0HJR1 (MmTX1) and C0HJR2 (MmTX2)].

[1]J.-P.R., J.R.S., and M.D.-B. contributed equally to this work.

[2]To whom correspondence may be addressed. Email: frankbosmans@jhmi.edu or pierre-edouard.bougis@univ-amu.fr.

This article contains supporting information online at www.pnas.org/lookup/suppl/doi:10.1073/pnas.1415488112/-/DCSupplemental.

snake venom and reveal the exciting prospect of discovering new tools to study these receptors.

Results

Identification of MmTX1 and MmTX2 in Coral Snake Venom. When using competitive binding assays on the Torpedo electric organ to search for novel α-neurotoxins active on nAChRs (22), we discovered a major but apparently inactive venom fraction from the Costa Rican coral snake *Micrurus mipartitus* (Fig. 1*A*). However, intracerebroventricular injection of this fraction into mouse brain [median lethal dose (LD_{50}) = 0.002 mg/kg] results in periods of reduced basal activity, followed by bursts of intense seizures. Intrigued by this observation, we purified this fraction (Fig. S1 *A–C*) and identified two amino acid sequences of 64 residues containing 10 cysteines each (Fig. 1*B*). Both peptides differ in one amino acid at position 33 with either an arginine (MmTX1, 7,205.0 Da) or a histidine (MmTX2, 7,186.0 Da).

A BLAST search revealed that MmTX1 and MmTX2 are novel members of the PATE-SLURP1-LYNX1-Ly-6/neurotoxin-like family (23–25) with a phylogeny pattern that classifies all homologous toxins into five clades (Fig. S2). The first clade consists exclusively of toxins found in *Micrurus* species, with MmTX1 and MmTX2 having the highest sequence identity. The availability of numerous three-finger snake toxin structures allowed us to reliably model MmTX1, using the MODELER program (27), which selected γ-bungarotoxin (PDB ID code 1MR6) and candoxin (PDB ID code 1JGK) as templates with a good ModPipe quality score of 1.5674 (Fig. S3). The predicted tertiary structure of MmTX1 fits within the three-fingered snake toxin family with one of the five disulfide bridges located in the first loop-finger. As such, MmTX1 can be classified as a member of the Elapid weak-toxin subgroup, of which the biological activity has not been defined (28).

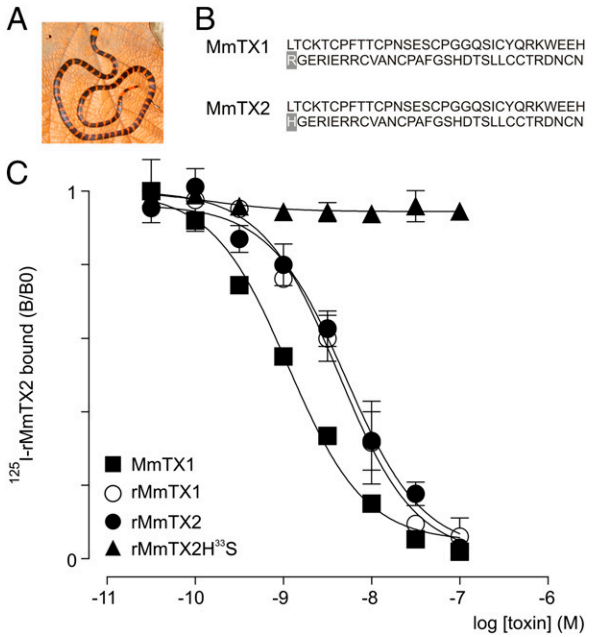

Fig. 1. Native and recombinant MmTX1 and MmTX2 are equally potent. (*A*) Picture of the Costa Rican coral snake *M. mipartitus* (provided by Alejandro Solórzano). (*B*) Primary amino acid sequences of MmTX1 and MmTX2. Note the different residue at position 33 (gray background). (*C*) Competition experiments for the binding of ^{125}I-rMmTX2 to synaptosomes with WT MmTX1, rMmTX1, rMmTX2, and the rMmTX2H^{33}S mutant. Lines represent a non-linear fit with constrained ^{125}I-rMmTX2-parameters (K_d = 0.51 nM and assay concentration 0.2 nM). Note that WT MmTX1, rMmTX1, and rMmTX2 are equally potent in displacing ^{125}I-rMmTX2, whereas rMmTx2H^{33}S is ineffective.

Therefore, resolving the working mechanism of MmTX1 may help pinpoint the primary molecular target of this toxin family.

Production of MmTX1 and MmTX2. *M. mipartitus* is a rare Costa Rican snake species that delivers small quantities of venom. Thus, we developed a periplasmic expression system with the goal of producing recombinant (r)MmTX1 and rMmTX2 (*Experimental Procedures*). The in vivo activity of rMmTX1 and rMmTX2 was assayed using microinjections into mouse brain and resulted in a LD_{50} of 0.027 mg/kg and 0.010 mg/kg, respectively (n = 9), an outcome that approximates that of the native fraction (LD_{50} = 0.002 mg/kg). Moreover, comparable behavioral signs including reduced activity combined with severe seizure events were noted. In addition to establishing a recombinant expression system, we synthesized (s)MmTX1, using an Fmoc strategy. Correct folding of the five disulfide bridges was achieved by using controlled redox buffering (*Experimental Procedures*). To verify proper toxin function, we injected sMmTX1 into mouse brain and found both a LD_{50} value similar to that of rMmTX1 (0.013 mg/kg) and an identical mouse behavioral phenotype. These results indicate that native, recombinant, and synthetic MmTX1 and MmTX2 are equally effective in influencing their target. Next, we tested whether these toxins bind to receptors within rat brain synaptosomes.

Binding of rMmTX1 and rMmTX2 to Rat Brain Synaptosomes. To assess the activity of rMmTX1 and rMmTX2 in synaptosomes, we performed competitive binding experiments between ^{125}I-rMmTX2 and wild-type (WT) MmTx2, rMmTx1, and rMmTx2 (Fig. 1*C*). The equilibrium inhibition constant (K_i) of WT MmTX2 (K_i = 0.8 nM; log K_i = −9.09 ± 0.07) is comparable to that found for rMmTX1 (K_i = 3.0 nM; log K_i = −8.52 ± 0.10) and rMmTX2 (K_i = 3.7 nM; log K_i = −8.44 ± 0.11). Moreover, no difference in K_i is observed between rMmTX1 and rMmTX2. Because a polar arginine found in the tip of the central loop determines α-neurotoxin efficacy toward nAChRs (29, 30), we examined whether the corresponding amino acid also contributes to the biological activity of rMmTx2. To this end, we mutated the endogenous histidine at position 33 in the apex of the second loop to the smaller polar residue serine (rMmTX2H^{33}S) and measured competitive binding with ^{125}I-rMmTX2. We found that the mutation impairs rMmTX2 function, implying both that this locus is vital for toxin activity and that rMmTX2 may bind to $GABA_A$ receptors with an orientation similar to that observed with α-neurotoxins and nAChRs (Fig. 1 *B* and *C*).

Next, we investigated the binding rate of ^{125}I-rMmTX2 to synaptosomes, using concentrations ranging from 1 to 4 nM (Fig. 2*A*) and fitting the data by a single exponential association curve. Plotting each observed kinetic constant against the respective ^{125}I-rMmTX2 concentration yields a second-order kinetic constant of association (k_{+1}) of 3.7 ± 0.5 × 10^6 M^{-1}·s^{-1} (Fig. 2*B*). The dissociation process of ^{125}I-rMmTX2 bound to synaptosomes was determined after the addition of a 1,000-fold excess of unlabeled rMmTX2 (Fig. 2*C*). Fitting the data with a single exponential decay curve results in a first-order kinetic constant (k_{-1}) of 0.0014 ± 0.0004 s^{-1} and a half time duration of ∼8 min, suggesting a very tight binding of the toxin to its target. From the ratio of both kinetic constants, we can deduce a true dissociation value ($K_d = k_{-1}/k_{+1}$) of 0.38 ± 0.05 nM. Finally, we conducted a saturation binding experiment at equilibrium, using ^{125}I-rMmTX2 concentrations up to 6 nM. Nonspecific binding was determined in the presence of a 1,000-fold excess of unlabeled rMmTX2 and subtracted to obtain specific binding data (Fig. 2*D*). The results of this experiment suggest the presence of a single class of non-interacting binding sites with a K_d of 0.51 ± 0.09 nM and a maximum capacity B_{max} of 264 ± 14 fmol/mg of synaptic protein.

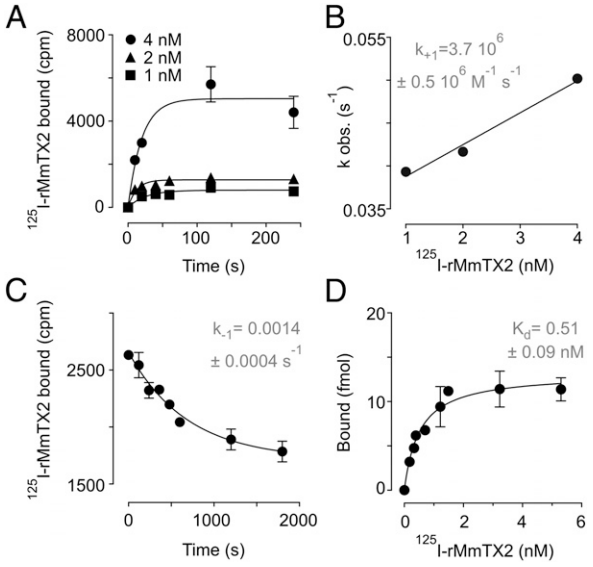

Fig. 2. Binding kinetics of rMmTX2 to rat brain synaptosomes. (*A*) Association kinetics of ^{125}I-rMmTX2 binding to synaptosomes. Shown are the association curves for ligand concentrations 1, 2, and 4 nM. Lines represent a nonlinear fit with a one-phase exponential association curve providing pseudo-first order association constants (k_{obs}) that are used in *B*. (*B*) The k_{obs} linear variation with 1-, 2-, and 4-nM ligand concentrations. Slope represents the association kinetic constant (k_{+1}; shown in inset). (*C*) Dissociation kinetics of ^{125}I-rMmTX2 from synaptosomes. Once the initial toxin binding is achieved, the addition of a 1,000-fold excess of unlabeled rMmTX2 reveals the time-course of toxin dissociation. Line represents a nonlinear fit with a one-phase exponential decay providing the shown rate constant (k_{-1}) and a $t_{1/2}$ of 478 s (~8 min). (*D*) Saturation binding isotherm of ^{125}I-rMmTX2 to synaptosomes. Nonspecific binding as determined in the presence of a 1,000-fold excess of unlabeled rMmTX2 has been subtracted. Line represents a nonlinear fit with one class of noninteracting binding sites giving an equilibrium binding constant (K_d) of 0.51 ± 0.09 nM and a maximum specific binding (B_{max}) of 264 ± 14 fmol/mg.

Biological Function of rMmTX1 Suggests $GABA_A$ Receptor Modulation. Both rMmTX1 and rMmTX2 evoke seizures when injected into mouse brain (LD_{50} = 0.010–0.027 mg/kg) but are inactive when injected i.v. at doses up to 1 mg/kg. This phenotype is distinct from that observed when administering α-neurotoxins that target nAChRs to produce a flaccid paralysis (31). Together, these assays suggest that MmTX1 and MmTX2 do not act on nAChRs but may affect structurally related $GABA_A$ receptors expressed in the central nervous system. In a biological context, the Costa Rican coral snake can feed on vermiform species that depend on $GABA_A$ receptors for locomotion (32). Altering receptor function by MmTX1 and MmTX2 envenomation may therefore result in prey paralysis. To test this hypothesis, we investigated the effect of rMmTX1 in the established *Caenorhabditis elegans* model, in which disruption of GABAergic neurotransmission induces simultaneous contractions of the body wall muscles (32). We found that topically applied rMmTX1 (30 μM) gradually paralyses *C. elegans* with a maximal effect at 1 h (Fig. S4). Conversely, the influence of rMmTX1 is alleviated in the *unc-49B* (e382/G189E) mutant, a *C. elegans* variant in which the gene encoding $GABA_A$ receptors is disrupted (33). This observation supports the notion that the Costa Rican coral snake can prey on soft-bodied animal phyla by targeting $GABA_A$ receptors. It is worth mentioning that paralysis still occurs at longer incubation times (>50 min) (Fig. S4), which can be attributed to a nonspecific effect of 30 μM rMmTX1 on other Cys-loop receptors present in *C. elegans* (34).

Binding of rMmTX2 to $GABA_A$ Receptors in Rat Brain Synaptosomes. In mammals, $GABA_A$ receptors are primarily found in the central nervous system. Thus, we set out to identify the primary target of rMmTX2 in GABA-depleted rat brain synaptosomes by carrying out competitive binding experiments with modulators of nAChRs, muscarinic (m)AChRs, $GABA_A$ receptors, GlyRs, glutamate receptors (GluRs), and acetylcholinesterase. Given its close structural relation to members of the α-neurotoxin family that bind to nAChRs, we initially investigated whether rMmTX2 competes with snake α-neurotoxins (Nmm I and α-bungarotoxin) (35, 36), as well as marine snail α-conotoxins (M1 and IM 1) (37, 38) and a plant toxin (d-tubocurarine) (39) (Fig. 3*A*). No competition is observed, suggesting nAChRs are indeed not the primary target of rMmTX2. Similarly, rMmTX2 does not compete with atropine, glycine, glutamate, and fasciculin Fas 2 (40), which target mAChRs, GlyRs, GluRs, and acetylcholinesterase, respectively. Finally, rMmTX2 does not displace cardiotoxin, a cytotoxic membrane-targeting peptide that also belongs to the three-finger α-neurotoxin structural family (Fig. 3*A*) (41).

We next examined whether ^{125}I-MmTX2 targets $GABA_A$ receptors in synaptosomes by conducting competitive binding experiments with seven compounds that bind to diverse regions on the receptor. Given the well-documented allosteric behavior of pentameric Cys-loop receptors on ligand binding (42–44), we may expect ^{125}I-MmTX2 to compete with agonists and antagonists, as well as allosteric modulators (Fig. 3*B*). We found that the competitive $GABA_A$ receptor antagonist gabazine is the most effective in reducing ^{125}I-MmTX2 binding (EC_{50} = 0.2 μM; log EC_{50} = −6.81 ± 0.03; n_H = 1.00 ± 0.07). In addition, the agonists GABA (EC_{50} = 2.7 μM; log EC_{50} = −5.56 ± 0.08; n_H = 0.99 ± 0.18) and muscimol (EC_{50} = 2.1 μM; log EC_{50} = −5.67 ± 0.09; n_H = 1.08 ± 0.24) reduce toxin binding to a similar extent. Moreover, the positive allosteric modulators diazepam (EC_{50} = 4.9 μM; log EC_{50} = −5.30 ± 0.04; n_H = −0.96 ± 0.07) and pentobarbital (EC_{50} = 4.8 μM; log EC_{50} = −5.32 ± 0.03; n_H = 0.98 ± 0.07) are equally potent in displacing ^{125}I-MmTX2. In contrast, the partial agonist isoguvacine (EC_{50} = 275 μM; log EC_{50} = −3.56 ± 0.10; n_H = 1.02 ± 0.29) is the least efficient in reducing ^{125}I-MmTX2 binding. Surprisingly, the noncompetitive channel blocker PTX (EC_{50} = 3.7 μM; log EC_{50} = −5.43 ± 0.07; n_H = +1.05 ± 1.16) markedly potentiates ^{125}I-MmTX2 binding to synaptosomes. To distinguish between effects of PTX on ^{125}I-MmTX2 binding site affinity and capacity, we repeated an experiment at equilibrium in the presence of a saturating PTX concentration (1 mM) (Fig. 3*C*). By comparing binding isotherm constants, we found that PTX potentiates ^{125}I-MmTX2 binding capacity without affecting toxin affinity (K_d with PTX = 0.76 ± 0.18 nM and B_{max} = 532 ± 33 fmol/mg of synaptosome protein, giving a ratio with/without PTX of 2.01). Finally, we assessed whether rMmTX1 has an effect on [^{3}H]muscimol binding. Because $GABA_A$ receptors possess both a high- and low-affinity muscimol binding site (45, 46), we conducted this experiment at saturating concentrations (40 nM). Using a nonlinear fit for an allosteric modulator (47), we found that rMmTX1 is able to compete with [^{3}H]muscimol with a K_d of 4.9 ± 0.2 nM, and only for about 40% of the total [^{3}H]muscimol binding capacity (Fig. 4), suggesting rMmTX1 may only influence one muscimol binding site. Altogether, our results indicate that rMmTX2, and by extension rMmTX1, preferentially targets $GABA_A$ receptors with high affinity. Moreover, a variety of allosteric and orthosteric compounds compete with ^{125}I-MmTX2 binding, whereas the pore-blocking molecule PTX doubles toxin-binding capacity without changing toxin affinity. This doubling can be interpreted as the appearance of a second toxin binding site on the same receptor molecule or a separate unmasking of a single binding site on receptors that lack this feature in the absence of PTX. Next, we explored toxin activity on mouse hippocampal neurons. Because rMmTX1, rMmTX2, and sMmTX1 have comparable effects in our mouse and binding assays, we consider both toxins as well as their synthesis route to be interchangeable.

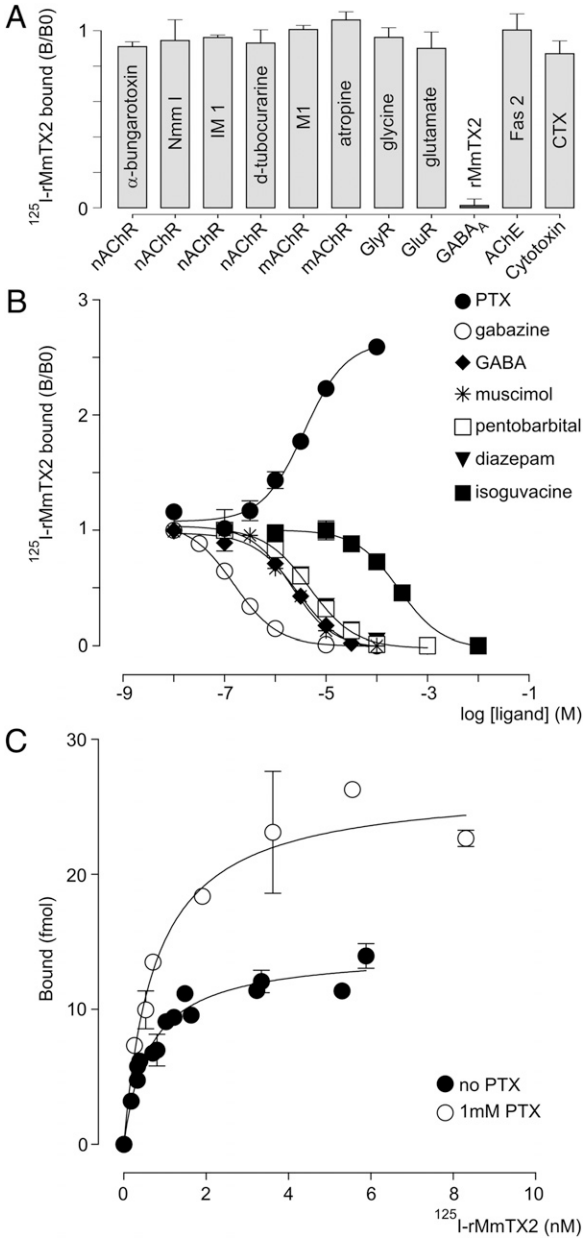

Fig. 3. Pharmacologic profiling of rMmTX2 . (*A*) Bar-plot of competition experiments between ^{125}I-rMmTX2 and a variety of ligands for binding to synaptosomes. The tested compounds are shown within the bar, and their primary target is indicated on the *x* axis. Concentrations used: all animal toxins 10 μM, (rMmTX2 100 nM), glycine 1 mM, glutamate 0.1 mM, atropine 1 μM, d-tubocurarine 10 μM. Diagram shows that none of the tested ligands competes with ^{125}I-rMmTX2 for binding to synaptosomes. (*B*) Competition experiments of ^{125}I-rMmTX2 with a variety of GABA$_A$ receptor modulators. Tested compounds are listed with their corresponding symbols. Lines represent a nonlinear fit with a sigmoidal dose–response curve (variable slope; HillSlope) to provide the EC_{50} values listed in the text. The only exception is PTX, which increases the binding of ^{125}I-rMmTX2. (*C*) Saturation binding isotherm of ^{125}I-MmTX2 on synaptosomes in the absence or presence of 1 mM PTX.

rMmTX1 Influences GABA$_A$ Receptor-Mediated Currents in Hippocampal Neurons. To test the biological activity of rMmTX1 on mouse brain hippocampal neurons, we first applied 100 nM in the absence of an agonist but observed no effect on GABA$_A$ receptors. In contrast, we see a potentiating effect of the toxin in the presence of a subsaturating concentration of 5 μM muscimol: rMmTX1 increases the amplitude of the GABA$_A$ receptor-mediated current elicited by 5 μM muscimol in a dose-dependent manner (Fig. 5*A* and Table S1). In the absence of rMmTX1, 100 nM muscimol fails to elicit a detectable current in 71% of neurons tested ($n = 7$). However, we observed a Cl^- current of 228 ± 30 pA when 100 nM muscimol is applied together with 100 nM rMmTX1 (Fig. 5*B*). In 43% of tested neurons ($n = 7$), 300 nM muscimol induces no response, whereas application of 300 nM muscimol together with 100 nM rMmTX1 generates a large inward current (439 ± 51 pA). In the remaining 57% of neurons, 300 nM muscimol induces a small inward current that is strongly potentiated by simultaneous application of 100 nM rMmTX1. In contrast to the potentiating effect of rMmTX1 in the lower range of muscimol concentrations, we do not observe a toxin-induced potentiation at muscimol concentrations greater than 10 μM (Fig. 5*B*). On determining the concentration-dependence of GABA$_A$ receptor currents by muscimol alone, we find an EC_{50} of 4.1 μM and an n_H coefficient of 1.4 (Fig. 5*C*), which is in agreement with reported values for GABA$_A$ receptors [5–24 μM and n_H between 1.1 and 1.6 (15)]. When surveying a range of muscimol concentrations in the presence of 100 nM rMmTX1, it is clear that the toxin causes GABA$_A$ receptor-mediated currents to increase about eightfold at low agonist concentrations, whereas saturating muscimol quantities suppress toxin effects (Table S2). From these data, the rMmTX1-induced portion of the current amplitude was determined and plotted versus muscimol concentration, thereby revealing that the half-maximal potentiating effect of 100 nM rMmTX1 is obtained at ~1 μM muscimol (Fig. 5*C*). Altogether, our data suggest that rMmTX1 potentiates GABA$_A$ receptor activation in a non-saturating concentration range of muscimol. However, an increase in inward Cl^- currents explains the rest behavior observed in mice receiving MmTX1/MmTX2 injection into the brain, but not the ensuing seizure episodes, which resemble those observed when inhibiting GABA$_A$ receptors with PTX. To further investigate the molecular mechanism underlying MmTX1/MmTX2 action, we tested the toxins on common GABA$_A$ receptor variants expressed in heterologous systems.

sMmTX1 Modulates Heterologously Expressed GABA$_A$ Receptors. We first assessed the effect of the toxin on HEK 293 cells transiently expressing the α1β2γ2 GABA$_A$ receptor, which is abundantly found in the hippocampus (48). When applying 300 nM muscimol in the presence of 100 nM sMmTX1, we observe an increase

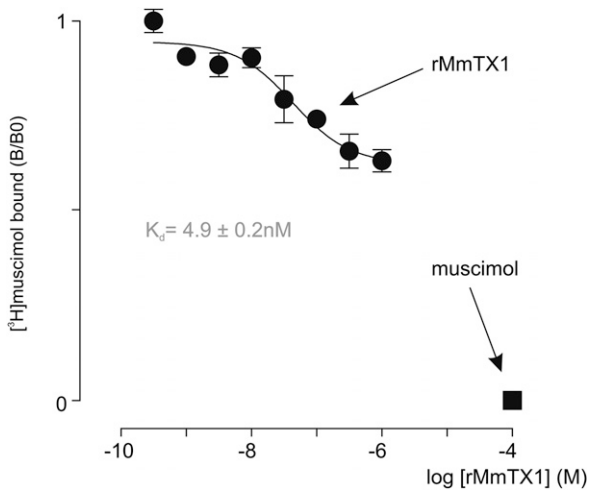

Fig. 4. [^{3}H]muscimol competition with rMmTX1 for binding to rat brain synaptosomes. rMmTX1 competes for binding with [^{3}H]muscimol. Line represents a nonlinear fit for the allosteric modulator with constrained [^{3}H]muscimol parameters (K_d = 1.75 nM and assay concentration 40 nM, implying that both GABA binding sites are occupied).

in the current of α1β2γ2 receptors by a factor of 2.7 ± 0.23 (n = 4; P = 0.0054). Similar to hippocampal neurons, the current elicited by 50 μM muscimol is not significantly altered by 100 nM toxin (factor of 1.0 ± 0.02; n = 8; P = 0.80), and as such, the potentiating effect of sMmTX1 is dependent on muscimol concentration. Increasing concentrations of sMmTX1 potentiate the $GABA_A$ receptor-mediated current amplitudes elicited by 3 μM muscimol by a similar degree: at 10 nM toxin, the current increases by a factor of 1.28 ± 0.12 (n = 10; P = 0.042); at 100 nM, it increases by 1.33 ± 0.13 (n = 10; P = 0.036); and at 300 nM, it increases by 1.60 ± 0.11 (n = 12; P = 0.0002). In addition, we observe a speeding up of receptor desensitization (the loss of current in the continued presence of agonist) when 100 nM toxin is present, whereas deactivation (the process by which currents return to baseline after agonist washout) is unaffected (Fig. 6*A*). This trend is also visible when 100 nM rMmTX1 is applied to cultured hippocampal neurons in the presence of 300 nM muscimol (Fig. 5*B*, *Center*). In contrast to synaptic $GABA_A$ receptors, which are transiently activated by high GABA concentrations (49), extrasynaptic $GABA_A$ receptors enable neurons to sense low ambient agonist concentrations present in the extracellular space to generate a form of tonic inhibition (50). Although these receptors commonly contain a δ or ε subunit, the observation that sMmTX1 is most effective at low muscimol concentrations suggests a possibility for the toxin to influence this persistent macroscopic conductance.

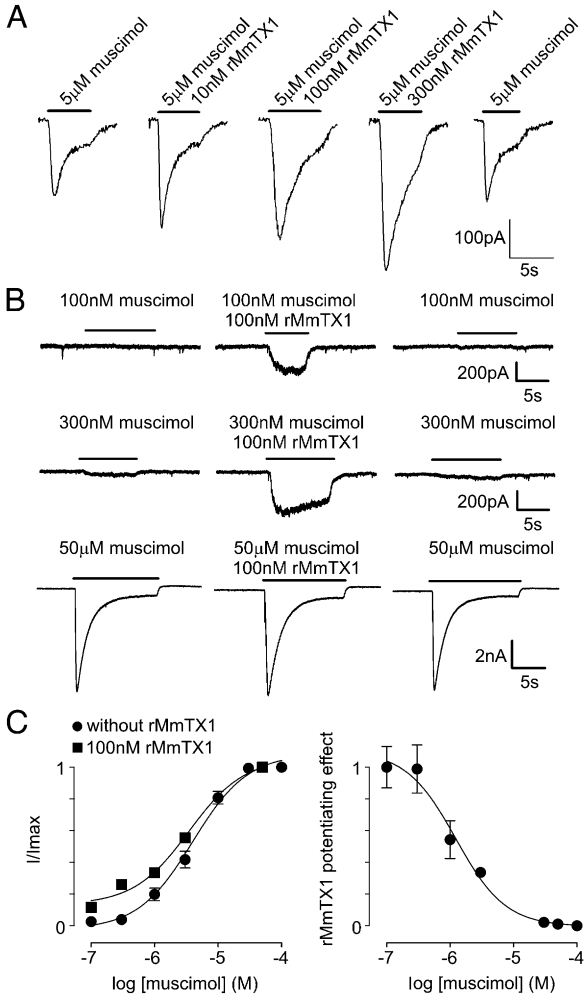

Fig. 5. Effect of rMmTX1 on hippocampal $GABA_A$ receptor currents. (*A*) Potentiation of the muscimol-induced $GABA_A$ receptor current depends on rMmTX1 concentration. Currents were elicited with 5 μM muscimol without and with increasing rMmTX1 concentrations. Membrane holding voltage was −70 mV. (*B*, *Upper*) Currents elicited with 100 nM muscimol (*Left*) followed by coapplication with 100 nM rMmTX1 (*Center*), and then without rMmTX1 (*Right*). (*Middle*) Currents elicited with 300 nM muscimol. (*Lower*) Currents elicited with 50 μM muscimol. Bars represent the duration of sample application. (*C*, *Left*) Dependence of the $GABA_A$ receptor current amplitude on muscimol concentration. A Hill equation was fitted to the data points (filled circles), yielding an EC_{50} of 4.1 μM and a Hill coefficient of 1.4. These data points and SEM were multiplied by the factor given in Table S2, yielding the rMmTX1-induced mean $GABA_A$ current increase (filled squares). (*Right*) Muscimol-dependent potentiating effect of rMmTX1 calculated as the toxin-induced current increase in relation to the total current amplitude. High muscimol concentrations abolish the potentiating effect with an IC_{50} of 1.1 μM.

To investigate the effect of sMmTX1 further, we expressed the α1β2γ2 $GABA_A$ receptor in *Xenopus* oocytes and assessed receptor desensitization and deactivation during 30-s toxin applications. Taking into account the complex gating mechanisms of rapidly activating $GABA_A$ receptors on agonist application and our relatively slow gravity-fed perfusion system, we did not expect to see a toxin-induced effect on Cl^- influx. However, 30-s toxin applications may still reveal alterations in receptor desensitization that occur at a slower rate compared with receptor activation (51, 52). Therefore, we set up a protocol consisting of two 30-s test applications of 5 μM muscimol separated by a 3-min washout period, followed by a 30-s 100 nM sMmTX1 application in concert with 5 μM muscimol and a washout phase. Under control conditions, α1β2γ2 $GABA_A$ receptors desensitize slowly in oocytes [single exponential fit yields a time constant (τ) of 48 ± 5 s; n = 3]; however, we observe a substantial increase in receptor desensitization in the presence of 100 nM sMmTX1 (τ = 25 ± 3 s; n = 3), whereas deactivation seems unaffected (Fig. 6*C*). As is typical with snake neurotoxins (53), sMmTX1 washout is very slow (Fig. 2*C*), and after 3 min, only a fraction of nondesensitized receptors can be activated again, an observation that fits well with our binding studies (Fig. 2*C*). When lowering the muscimol concentration to 300 nM, we observe a similar effect of 100 nM sMmTX1 on receptor desensitization (Fig. 6*E*). Interestingly, this outcome is also achieved when expressing only the α1β2-containing receptor in oocytes (Fig. 6*F*), suggesting that in contrast to benzodiazepines, the γ2 subunit is not required for sMmTX1 efficacy. Moreover, experiments with other subunit compositions (α2β3γ2, α3β2γ2, α5β3γ2, and α1β3) expressed in oocytes suggest an important role for the α1 subunit in $GABA_A$ receptor sensitivity to 100 nM sMmTX1 (Fig. S5). However, future experiments will have to determine whether other α subunits are also susceptible to toxin binding at a range of concentrations in complex systems, as context-dependent variations in pharmacologic sensitivity of Cys-loop receptors have been documented (54). Altogether, our results with heterologously expressed $GABA_A$ receptors suggest that sMmTX1 initially increases Cl^- influx, leading to membrane hyperpolarization. In addition, receptor desensitization is promoted, which results in a substantial decrease of functioning $GABA_A$ receptors. One explanation for this seemingly complex effect is that, similar to benzodiazepines, sMmTX1 allosterically increases $GABA_A$ receptor susceptibility to low concentrations of muscimol, which in turn results in a potentiation of macroscopic conductance and desensitization (55, 56).

sMmTX1 Function Is Influenced by Mutations in Loop-C of the α1 Subunit. Accumulating evidence obtained from nAChRs establishes a vital role for loop-C within the α subunit in determining receptor sensitivity to α-neurotoxins (57, 58). Subsequently, we hypothesized that sMmTX1 interacts with the corresponding region in the α1 subunit of $GABA_A$ receptors expressed in oocytes (Figs. S3 and S5). Aligning the primary sequence of α1–6 reveals unique residues in loop-C of the α1 subunit, of which we chose to

mutate ^{228}Gly (G) and ^{231}Gln (Q) to a Glu (E) and Lys (K), respectively. When expressed in oocytes, this $\alpha1_{EK}\beta2\gamma2$ receptor mutant is functional; however, two 5 μM muscimol applications separated by a 3-min washout period reveal a consistent current rundown (Fig. S6; $n = 4$). Contrary to experiments with the WT α1 subunit (Fig. 6*C*), 100 nM sMmTX1 does not increase mutant receptor desensitization or significantly influence its response to 5 μM muscimol after toxin washout ($n = 4$). In the presence of 300 nM muscimol, sMmTX1 still reduces the macroscopic conductance of the $\alpha1_{EK}\beta2\gamma2$ receptor, yet toxin washout is markedly faster compared with WT (Fig. S6). Although the double mutation does not abolish toxin effect, our observations do suggest an involvement for loop-C in sMmTX1 action. Nonetheless, additional mutagenesis experiments are required to delineate the complete binding site of sMmTX1 within the α1 or other subunits.

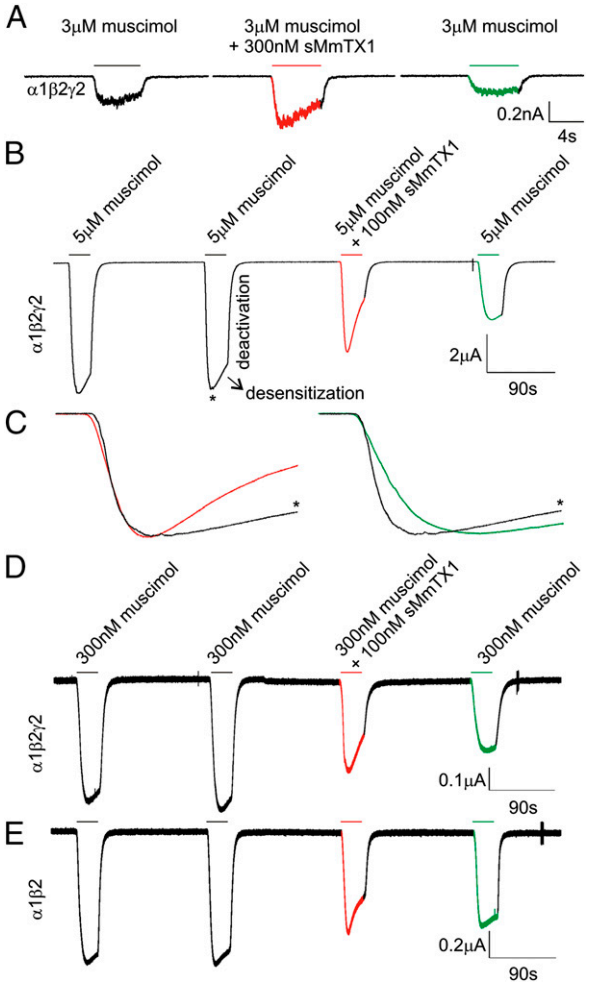

Fig. 6. Effect of sMmTX1 on $\alpha1\beta2\gamma2$ $GABA_A$ receptor currents. (*A*) A muscimol concentration of 3 μM activates $\alpha1\beta2\gamma2$ $GABA_A$ receptors expressed in HEK 293 cells (*Left*) held at a membrane voltage of −70 mV. When coapplying 300 nM sMmTX1, currents are potentiated and receptor desensitization tends to accelerate (*Middle*). Toxin washout is shown on the right. (*B*) Expression of the $\alpha1\beta2\gamma2$ receptor in *Xenopus* oocytes held at a membrane voltage of −70 mV. Protocol consists of two 30-s test applications of 5 μM muscimol separated by a 3-min washout period, followed by 100 nM sMmTX1 application together with 5 μM muscimol. Under control conditions, receptors desensitize with a time constant of 48 ± 5 s ($n = 4$). In the presence of 100 nM sMmTX1, the time constant is 25 ± 2 s ($n = 4$). sMmTX1 washout is slow, and after 3 min, only a fraction of the receptors can be reactivated. Moreover, available receptors activate more slowly compared with control, suggesting toxin is still bound. (*C*) Close-up of the red and green region indicated in *B* normalized to the control peak (indicated with an asterisk). (*D*) When lowering the muscimol concentration to 300 nM, a similar effect of 100 nM sMmTX1 on receptor desensitization is observed ($n = 4$). (*E*) Similar to the $\alpha1\beta2\gamma2$ receptor, the $\alpha1\beta2$-containing receptor expressed in oocytes held at −70 mV is sensitive to 100 nM sMmTX1. A representative example of four recordings is shown.

sMmTX1 Alters Spontaneous Hippocampal Neuron Activity. To assess the influence of sMmTX1 on the activity of a neuronal network, we monitored Ca^{2+} oscillations of hippocampal neurons in culture without and in the presence of toxin. Taking into account the $GABA_A$ receptor developmental switch from excitatory to inhibitory, we used cells that were kept in culture for 3 wk. Thus, the transition to inhibitory function should be complete (59). Cells were incubated in Fluo-4 AM and then subjected to fluorescent time-lapse imaging to measure Ca^{2+} oscillations. Separate applications of 300 nM muscimol or 100 nM sMmTX1 have no apparent effect on the frequency of Ca^{2+} spikes (Fig. 7 *A*, *B*, and *D*) compared with cells perfused with extracellular saline solution [98.0 ± 4.8% ($n = 9$) and 105.8 ± 4.0% ($n = 9$), respectively]. However, coapplication of 300 nM muscimol and 100 nM sMmTX1 produces a short but substantial inhibition of Ca^{2+} oscillations, thereby supporting the observation of $GABA_A$ receptor activation, which in turn inhibits network activity. This inhibitory period is followed by a large increase in the frequency of Ca^{2+} oscillations (171.7 ± 8.4%; $n = 25$; $P < 0.0001$) (Fig. 7 *C* and *D*). Although we cannot exclude the possibility of sMmTX1 interacting with other receptors in a noncompetitive manner, the observed decrease followed by an increase in network activity supports the hypothesis that sMmTX1 binds tightly to $GABA_A$ receptors to increase agonist sensitivity, which initially activates and then desensitizes the receptors for as long as the toxin is bound. To further investigate the influence of sMmTX1 on network activity, we recorded spontaneous electrophysiologic activity in hippocampal neurons. Cells treated with sMmTX1 show a substantial increase in the frequency of action potential (AP) firing (Fig. 7*F* and Fig. S7*A*; $n = 5$). No significant changes are detected in other parameters, such as AP amplitude ($P = 0.1043$; $n = 5$) or time to peak ($P = 0.3185$) (Fig. S7*A*). Interestingly, most of these events occur in bursts that resemble epileptiform activity. Similarly, spontaneous activity assessed by voltage-clamp recordings (Fig. 7*E*; $n = 5$) show a considerable increase in the duration of burst-like postsynaptic currents compared with mostly single spontaneous events under control conditions. Moreover, each burst is followed by a silence period, as can be clearly seen by an increase in the time between firing (Fig. 7*E*). We examined how these observations compare with the effect of the pore-blocking PTX compound at 100 μM, a commonly used concentration. Although PTX also produces burst-like currents under voltage-clamp recordings (Fig. 7*G*), the AP frequency increases more dramatically compared with sMmTX1. Moreover, these events present themselves as single APs or bursts with a much longer duration and a shorter silence interval (Fig. 7*G*). To get a better insight into the biological working mechanism of sMmTX1, we set up a scenario in which we continuously perfused hippocampal cells with toxin and applied 30-ms puffs of 300 nM muscimol every 5 s. Under these conditions, the toxin should be continuously bound to the receptor, whereas the agonist is washed out after each application. Consistent with a mechanism in which sMmTX1 increases agonist efficacy to induce long-term desensitization, ensuing voltage-clamp recordings indeed show a significant decrease in the currents elicited by the muscimol puff in presence of the toxin (−53.3 ± 3.4 to −34.5 ± 1.3; $P < 0.0001$) (Fig. S7*B*). There are no apparent kinetic differences, as judged by the rise and decay of normalized currents (Fig. S7*B*). To isolate the GABA component of the postsynaptic response, we also measured mini inhibitory postsynaptic currents (mIPSCs) in neurons perfused with extracellular solution, followed by a muscimol/sMmTX1 treatment. Supporting

the notion that sMmTX1 targets $GABA_A$ receptors, we detected a 48.4 ± 4.7% decrease in the amplitude of spontaneous events (Fig. S7*C*). Overall, these data support the hypothesis that sMmTX1 acts as an allosteric modulator of $GABA_A$ receptors and help explain the intermittent seizures observed in animals on toxin injection into the brain.

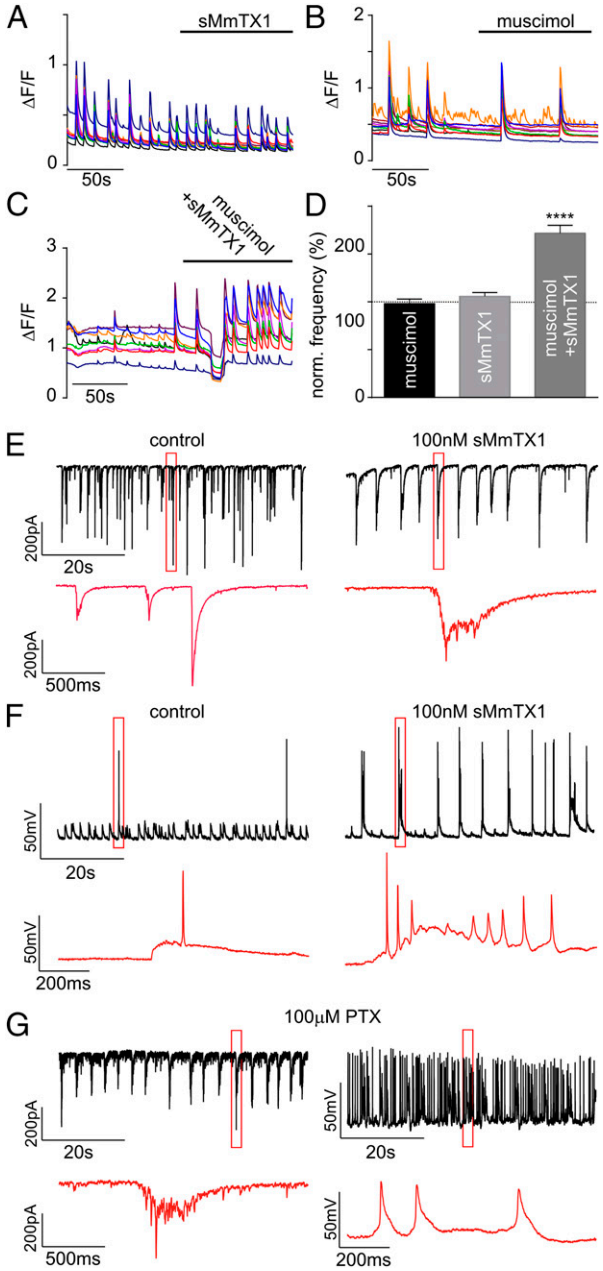

Fig. 7. sMmTX1 influences hippocampal network function. (*A*) sMmTX1 by itself does not affect the frequency of Ca^{2+} oscillations. (*B*) 300 nM muscimol does not have a detectable effect on the frequency of Ca^{2+} oscillations. (*C*) When applied together with muscimol at 300 nM, sMmTX1 produces a short inhibition of network Ca^{2+} oscillations, followed by a marked increase in spike frequency. (*D*) Quantification of *A*–*C* represented as a percentage variation of the Ca^{2+} oscillation frequency with respect to cells perfused with extracellular solution (100%, dotted line). Data are presented as mean ± SEM *t* test: $P < 0.0001$ for muscimol + sMmTX1 application (****). (*E* and *F*) Representative traces of recordings of neurons perfused with artificial cerebrospinal fluid (*Left*) or muscimol-sMmTX1 (*Right*), under voltage- and current-clamp configuration, respectively ($n = 5$). Zoomed-in areas indicated by the red rectangle in traces *E* and *F* are shown in red in the lower panel in each figure. (*G*) Representative traces of recordings of neurons perfused with 100 μM PTX under voltage- (*Left*) and current- (*Right*) clamp configuration, respectively ($n = 5$). Zoomed-in areas indicated by the red rectangle are shown in red in the lower panel.

Discussion

For many years, animal venoms have been a valuable source of toxins for studying the functional properties and pharmacologic sensitivities of receptor and ion channel families (60–62). However, no animal toxins have been identified that selectively target $GABA_A$ receptors at subnanomolar concentrations. [Several reports suggest that Waglerin-1 and α-bungarotoxin are non-selective $GABA_A$ receptor modulators that principally influence nAChRs (63, 64).] However, the discovery of such ligands for this protein family may substantially advance research efforts geared toward elucidating their physiologic role or produce lead compounds for drug design. To fill this gap, we explored the venom of Costa Rican coral snakes that can feed on worms in which GABA may function as a locomotion neurotransmitter (32, 65). We isolated two toxins, micrurotoxins MmTX1 and MmTX2, which make up ∼50% of the total venom quantity (Fig. 1*A* and Figs. S1 and S2). Given the sequence homology with other three-finger toxins isolated from snake venoms, it is intriguing that MmTX1 and MmTX2 do not bind to nAChRs (Fig. 3*A*). Similar to α-neurotoxins, MmTX1 and MmTX2 possess a functionally important and evolutionary conserved basic residue at position 33 that anchors the α-neurotoxin to the receptor (30). However, substantial amino acid sequence differences in the charge distribution of the apex within loop I, and to a lesser extent loop III, may contribute to an altered selectivity pattern (Fig. S3). Because endogenous toxin-like ion channel modulators are also found within this peptide family (25), a compelling hypothesis is that MmTX-like peptides may be present in the brain, where they act as endogenous $GABA_A$ receptor modulators.

MmTX1/MmTX2 injection into mouse brain causes periods of reduced activity, followed by stages of intense seizures, but they have no effect when injected intravenously. This observation suggests an interaction between MmTX1/MmTX2 and $GABA_A$ receptors, but not nAChRs. Indeed, extensive binding and competition studies on rat brain synaptosomes reveal that MmTX1 and MmTX2 bind to $GABA_A$ receptors with subnanomolar affinity (Fig. 3*B*). Moreover, neither toxin competes with a variety of ligands that bind to nAChRs, mAChRs, GlyR, GluRs, and acetylcholinesterase (Fig. 3*A*). When assaying toxin activity on adult hippocampal neurons isolated from mice, we find that 100 nM rMmTX1 has no effect unless administered together with a $GABA_A$ receptor agonist such as muscimol. At low agonist concentrations, brief applications of 100 nM rMmTX1 potentiate $GABA_A$ receptor-mediated currents, whereas this effect is lost at higher muscimol concentrations, thereby suggesting a role for extrasynaptic $GABA_A$ receptors in the observed mouse behavioral effects on toxin application (Figs. 5 and 6*B*) (50). This potentiation is also present when subjecting $\alpha1\beta2\gamma2$ $GABA_A$ receptors expressed in HEK 293 cells to the same treatment (Fig. 6*A*). When coapplying muscimol and 100 nM sMmTx1 for longer periods to $\alpha1\beta2\gamma2$ $GABA_A$ receptors expressed in *Xenopus* oocytes, we observe a substantial increase in the rate of desensitization (Fig. 6 *C*–*F*). Even though extending these results to a complex neuronal network is not straightforward, our observations may account for the mouse phenotype in which toxin injection into the brain causes an initial membrane hyperpolarization that decreases neuronal excitability. Hereafter, accelerated long-term receptor desensitization prevents $GABA_A$ receptors from controlling membrane voltage, resulting in increased electrical activity and seizures. Correspondingly, hippocampal neuron measurements reveal an initial decrease in spontaneous spiking, followed by intense activity on coapplication of muscimol and 100 nM sMmTx1 (Fig. 7).

MmTX1 and MmTX2 enhance current amplitude only in the presence of a nonsaturating concentration of agonist (Fig. 6*B*).

Moreover, rMmTX2 competes for binding to $GABA_A$ receptors with orthosteric effectors such as gabazine and isoguvacine, a positive allosteric modulator of the benzodiazepine binding site (diazepam), and pentobarbital, a barbiturate of which the binding site differs from that of GABA and benzodiazepines (66). Taking into account that GABA binds to two extracellular β^+/α^- interfaces, benzodiazepines interact with the $\alpha^+/\gamma2^-$ interface, and the γ2 subunit is not required for MmTX1 activity, it is possible that the remaining α^+/β^- interface may be involved in toxin action. This relatively unexplored binding site is similar to that of benzodiazepines and is greatly influenced by the particular α subunit type present in the receptor (26). In concert, sMmTX1 activity in oocytes is altered by mutations in loop-C of the α1 subunit (Fig. S6). This particular component is also found in δ or ε subunits containing extrasynaptic $GABA_A$ receptors that are exposed to low ambient agonist concentrations (50). Therefore, elucidating the mechanism underlying the biological action of MmTX1/MmTX2 will require a precise delineation of the targeted subunits.

On a molecular level, one possible mode of action is that MmTX1 and MmTX2 allosterically increase receptor affinity for the agonist, thereby potentiating receptor opening and macroscopic desensitization. This working mechanism resembles that of benzodiazepines, which enhance receptor susceptibility ($K_d = k_{-1}/k_{+1}$) for GABA by decreasing the unbinding (off) rate (k_{-1}) and subsequently slowing the deactivation process (55). Although we cannot exclude a mixed mechanism that involves changes in both k_{-1} and k_{+1}, sMmTx1 does not seem to influence deactivation (Fig. 6), which would imply a mechanism geared toward increasing agonist binding (on) rate (k_{+1}); that is, to facilitate GABA access to its binding pocket. Notably, benzodiazepines possess a fast off rate (seconds), whereas MmTX1 and MmTX2 bind very tightly to $GABA_A$ receptors ($t_{1/2}$ of ~8 min). This divergence may relate to the long-term decrease in macroscopic conductance induced by sMmTX1, which can help explain the observed seizures in mice (Fig. 6 *C–F* and Fig. S7). It is also worth mentioning that alternative mechanisms of action cannot be ruled out. For one, toxin-induced $GABA_A$ receptor opening may trigger a hyperpolarization-activated excitatory conductance to generate rebound APs (67). Also, depolarizing responses to GABA have been reported in specific interneuron networks (68, 69). Although more experiments are needed to determine the precise mechanism underlying MmTX1 and MmTX2 biological activity, the discovery of a class of allosteric modulators interacting with the α^+/β^- interface markedly enriches $GABA_A$ receptor pharmacology.

Overall, the identification of $GABA_A$ receptor-targeting toxins in animal venom provides a conceptual example for discovering novel ligands to study this receptor family. Moreover, successful production of MmTX1 and MmTX2 will be valuable to further optimize their subtype selectivity and potency. In a broader context, both toxins provide tools to evoke seizures in assays designed to test antiepileptic drugs or as lead molecules for therapeutics that modulate $GABA_A$ receptor activity through a novel binding site.

Experimental Procedures

Bioassays. Lethality tests were performed using male Swiss mice (n = 48; weight: 18 ± 3 g) by s.c. or intracerebroventricular injections, as described previously (70). Experiments were carried out in accordance with European Union Directive 2010/63/EU.

Purification and Production of MmTX1 and MmTX2. MmTX1 and MmTX2 were purified from *M. mipartitus* venom from Costa Rica (family Elapidae, genus *Micrurus*; also referred to as *Micrurus multifasciatus*) (71), obtained from specimens maintained at the Serpentarium of Instituto Clodomiro Picado, by using a two-step HPLC protocol. First, 10 mg water-dialyzed venom (Spectra/Por 3) was loaded on a 10 × 250 mm 5 μm ultrasphere C8 column (Beckman) and eluted with a 8–35% (vol/vol) linear gradient of acetonitrile in 0.15 M ammonium formate at pH 2.7 at a flow rate of 5 mL/min. Next, the fraction at 58.70 min was transferred to a cation exchange 7.5 × 75 mm TSKSP-5 PW column (Beckman) and eluted after a 10-min step with a 0–30% linear gradient of 0.5 M ammonium acetate in 0.005 M ammonium acetate at pH 8.0 at a flow rate of 0.5 mL/min. Edman sequencing was carried out on a cysteine-reduced and s-carboxymethylated derivative (22). Toxin molecular masses were determined using electrospray ionization quadripole time of flight Ultima (Waters) with MaxEnt for spectra deconvolution. BLAST and PHYLIP (72) were used to construct a phylogenetic tree. Recombinant expression of MmTX1/MmTX2 was performed using a synthetic gene, and site-directed mutagenesis was carried out with the quick-change mutagenesis kit (Stratagene). All constructs were sequenced and expressed in *E. coli* HB 101 (Promega) as a fusion protein with the ZZ domain, a synthetic IgG-binding domain of protein A (73), using the vector pEZZ 18 Protein A Gene Fusion Vector (GE Healthcare). Fusion proteins were purified on an IgG-Sepharose column (GE Healthcare) and toxin-moiety kept free from the ZZ domain, using cyanogen bromide (74). The reaction product was loaded on a HPLC 4 × 250 mm 5 μm ultrasphere C18 column (Merck) at 10% (vol/vol) acetonitrile in 0.1% (vol/vol) TFA/H_2O, and then eluted with successive linear acetonitrile gradients, 10–20% in 5 min, 20–40% in 60 min, and 40–60% in 10 min. Toxin retention time was 26 min, and fusion protein was 38 min. Except where indicated, all chemicals were purchased from Sigma-Aldrich. sMmTX1 was chemically synthesized (Synprosis), using standard solid-phase peptide synthesis methodology and Fmoc chemistry on preloaded Fmoc-amino acid-Wang resin. Crude peptide was HPLC-purified on a RP-C18 column, using a 10–50% linear gradient of 0.1% TFA/acetonitrile in 0.1% aqueous-TFA. The 5-disulfide bridges were allowed to fold in a 100 mM Tris·HCl buffer, 1 mM EDTA, at pH 9.0, adding a combination of GSSG/GSH in a 1 mM/2 mM ratio and sMmTX1 at a concentration of 20 μM. The reaction was performed overnight under nitrogen. Next, a cation exchange concentration step was performed on a Mono S HR 5/5 column (GE Healthcare), using a 20-mL ammonium acetate elution gradient from 10 mM, at pH 5.5, to 2 M, at pH 5.1. Hereafter, a desalting purification step was performed by HPLC, as stated earlier.

Template-Based 3D Modeling. Homology modeling of MmTX1 was performed with MODELER (27), using ModWeb Server version SNV.r1368M within ModBase (75). Selected options were best-scoring model, longest well-scoring model, and slow search speed. Models with the highest ModPipe Protein Quality Score were selected. Visualization and drawing of selected models were accomplished with UCSF Chimera (76).

***Caenorhabditis elegans* Assay.** *C. elegans* WT worms and the *unc-49B* (e382/G189E) mutant (32, 33) were studied at the L4 stage of their live cycle. In each essay, 10 worms were incubated in 10 μL phosphate buffer (1 mM $CaCl_2$, 1 mM $MgSO_4$, 5 mM KH_2PO_4, at pH 6.0, adjusted with KOH, and 0.05% Tween20) in the absence (control) or the presence of 30 μM sMmTX1. Every 10 min, worms were visualized using a dissecting stereomicroscope and checked for mobility using a platinum wire. Results are shown as percentage of worms showing paralysis ± SEM (n = 3).

MmTX2 Iodination and Pharmacologic Experiments. $Na^{125}I$ and [^{3}H]muscimol were obtained from PerkinElmer, and isoguvacine from Peninsula laboratories. All other reagents were from Sigma-Aldrich. MmTX2 was radioactively labeled by lacto-peroxidase-catalyzed iodination (77) with specific activities of 900 Ci/mmol. Synaptosome fractions (P2) of Wistar rat brains were prepared as described previously (78) and stored in liquid nitrogen. Synaptosomes were lysed on ice by dilution into 15 volumes of hypotonic buffer 10 mM Tris, 1 mg/mL BSA, at pH 7.4, kept 30 min at 4 °C, and then pelleted at 12,500 × g, 20 min, at 5 °C. This protocol was run twice to remove endogenous GABA. Binding experiments were performed in 1.5-mL tubes in buffer 10 mM Tris, 100 mM NaCl, 1 mg/mL BSA, at pH 7.4, 50 μg synaptosome protein. Before checking radioactivity, tubes were centrifuged for 3 min at 13,000 × g and washed twice with iced buffer. The incubations were performed at 37 °C (^{125}I-MmTX2) or 4 °C ([^{3}H]muscimol). Experiments were carried out in triplicate and repeated at least twice. Data analysis and linear and nonlinear curve fitting were performed using GraphPad PRISM. Data are reported as mean ± SEM.

Heterologous Expression of $GABA_A$ Receptors in HEK 293 Cells. cDNA of the rat $GABA_A$ receptor α1 subunit was subcloned into the pBK expression vector, cDNA of the rat β_2 and γ_2 subunits was subcloned into the pCIS vector, and GFP cDNA was subcloned into the pcDNA3 vector. HEK 293 cells were cultivated in DMEM/Ham's F-12 medium containing 1% penicillin/streptomycin/L-glutamine and 10% (vol/vol) FBS at 37 °C in a water-saturated atmosphere

of 95% air and 5% CO_2. Cells were placed on poly-L-lysine-coated glass coverslips and transfected using the Ca^{2+} phosphate method. Successfully transfected cells were detected by GFP fluorescence.

Electrophysiologic Recording from Hippocampal and HEK 293 Cells. Hippocampal cells and HEK 293 cells transfected with the $\alpha1\beta2\gamma2$ $GABA_A$ receptor were patch-clamped under a water-immersed 40× objective of a Zeiss Axioskop 2 FS Plus. Borosilicate glass capillaries (Harvard Apparatus) were pulled (P-97 puller; Sutter Instruments) and had a resistance of 3–5 MΩ when filled with the internal solution. Membrane currents were recorded using Pulse and Patchmaster software (HEKA) in combination with an EPC-9 patch-clamp amplifier (HEKA). Data were low-pass filtered at 2.9 kHz. Only data from recordings with an access resistance <20 MΩ were evaluated. Data were analyzed using Fitmaster (HEKA), Igor Pro-6.03 (Wavemetrics), and Excel (Microsoft). Averaged values are given as mean ± SEM. Hippocampal cell cultures were prepared from P1 mice (C57Bl6J), following the procedure as described (79). Whole-cell patch clamp experiments were performed on hippocampal neurons (DIV 14) at room temperature (21–23 °C), and the holding potential was adjusted to −70 mV. The extracellular solution used in experiments with hippocampal neurons contained (in mM): 143 NaCl, 5 KCl, 0.8 $MgCl_2$, 1 $CaCl_2$, 10 Hepes, 5 glucose, 0.5 μM TTX, 10 μM CNQX (6-cyano-7-nitroquinoxaline-2,3-dione), and 20 μM APV (2-amino-5-phosphonovaleric acid), at a pH adjusted to 7.3 with NaOH. In experiments with HEK 293 cells, the same extracellular solution was used without TTX, CNQX, and APV. The pipette solution contained (in mM): 140 CsCl, 1 $CaCl_2$, 1 $MgCl_2$, 11 EGTA, 5 Hepes, at a pH adjusted to 7.2 with CsOH. Except where indicated, all chemicals were purchased from Sigma. For recordings in Fig. 7, artificial cerebrospinal fluid solution contained (in mM): 140 NaCl, 5 KCl, 2 $CaCl_2$, 2 $MgCl_2$, 10 Hepes, and 10 Glucose (pH 7.3, adjusted with NaOH). Recordings were performed with an Axopatch 200B amplifier equipped with Digidata 1440 and pClamp 10 (Molecular Devices). Current clamp whole-cell recordings were done using borosilicate glass pipettes (4–6 MΩ) filled with internal solution containing (in mM): 135 K-gluconate, 20 KCl, 10 Hepes, 4 Mg-ATP, 0.3 Na_2GTP, and 0.5 EGTA.

Electrophysiologic Recording from *Xenopus* Oocytes. Each rat $GABA_A$ receptor subunit as well as the $\alpha1_{EK}\beta2\gamma2$ mutant was expressed in *Xenopus* oocytes from which the vitellin membrane was removed manually. The DNA sequence of all constructs was confirmed by automated DNA sequencing before further use. cRNA was synthesized using T7 polymerase (Life Technologies) after linearizing the DNA with appropriate restriction enzymes. Channels were expressed in oocytes, and currents were studied after 1–2-d incubation after cRNA injection (incubated at 17 °C in 96 mM NaCl, 2 mM KCl, 5 mM Hepes, 1 mM $MgCl_2$, 1.8 mM $CaCl_2$, and 50 μg/mL gentamicin, at pH 7.6 with NaOH), using two-electrode voltage-clamp recording techniques (OC-725C; Warner Instruments), with a 150-μL recording chamber. Heterologous $GABA_A$ receptor manipulations were achieved using previously reported procedures (16, 80). Microelectrode resistances were 0.5–1 MΩ when filled with 3 M KCl. The external recording solution contained (in mM) 100 NaCl, 5 Hepes, 1 $MgCl_2$, and 1.8 $CaCl_2$ at pH 7.6 with NaOH. All experiments were performed at room temperature (~22 °C). Off-line data analysis and statistics were performed using Clampfit10 (Molecular Devices), Excel (Microsoft Office), and Origin 8 (OriginLab).

Calcium Imaging of Hippocampal Neurons. Hippocampi were obtained from Sprague–Dawley rat embryos at embryonic day 18, treated with papain (Worthington Biochemical), and dissociated with a pipette. Cells were plated over coverslips coated with Laminin (Life Technologies) and poly-D-Lysine (Sigma-Aldrich). Astrocyte beds were prepared at a density of 80,000 cells/mL and cultured in DMEM (Life Technologies) with 10% (vol/vol) FBS, 6 mM glutamine in 5% CO_2 at 37 °C. Neurons were plated over the course of 14 days in vitro confluent astrocyte beds at a density of 150,000 cells/mL and cultured for 3 weeks in Neurobasal supplemented with B27 and 2 mM GlutaMax. Neurons were incubated with 2 μm Fluo-4 AM (Life Technologies) for 15 min. The images were obtained with an Olympus BX51WI microscope equipped with a 40× immersion lens and a Lambda DG-4 Ultra-High-Speed Wavelength Switching Illumination System (Sutter Instruments), using a CCD camera (Hamamatsu) at 2 Hz. The recording chamber was perfused at 2 mL/min at 32 °C with artificial cerebrospinal fluid containing (in mM): 140 NaCl, 5 KCl, 2 $CaCl_2$, 2 $MgCl_2$, 10 Hepes, and 10 glucose (pH 7.3, adjusted with NaOH). Muscimol and sMmTX1 were prepared fresh in recording buffer at 300 nM and 100 nM, respectively. Calcium spikes were analyzed with MiniAnalysis (Synaptosoft). Values were expressed as percentage variation on the average frequency of calcium spikes of treated versus control neurons. Data are presented as mean ± SEM. Statistical analysis was performed using GraphPad PRISM. Data were analyzed with paired Student's test.

ACKNOWLEDGMENTS. We acknowledge M. F. Martin-Eauclaire (Aix Marseille Université) for recognizing the toxin-evoked epileptic phenotype in mice and for help with radioactive labeling of toxins. We thank O. Vargas and S. Conrod (Aix Marseille Université) for their involvement in toxin purification, R. Schlichter (Université de Strasbourg) for initial electrophysiology recordings, Madeleine Garcia (Aix Marseille Université) for *C. elegans* experiments, Yvonne Pechmann (University of Hamburg) for help with $GABA_A$ receptor expression in HEK 293 cells, C. Czajkowski (University of Wisconsin–Madison), R. L. Macdonald (Vanderbilt), D. Bowie (McGill), and D. S. Weiss (University of Texas Health Science Center–San Antonio) for sharing $GABA_A$ receptor clones, as well as C. J. McBain (NIH) for helpful discussions. A picture of *Micrurus mipartitus* (as seen in Fig. 1*A*) was provided by Alejandro Solórzano. This research was supported by the Centre National de la Recherche Scientifique.

1. Sieghart W (2006) Structure, pharmacology, and function of $GABA_A$ receptor subtypes. *Adv Pharmacol* 54:231–263.
2. Ferando I, Mody I (2014) Interneuronal $GABA_A$ receptors inside and outside of synapses. *Curr Opin Neurobiol* 26:57–63.
3. Moss SJ, Smart TG (2001) Constructing inhibitory synapses. *Nat Rev Neurosci* 2(4): 240–250.
4. Stein V, Nicoll RA (2003) GABA generates excitement. *Neuron* 37(3):375–378.
5. Hines RM, Davies PA, Moss SJ, Maguire J (2012) Functional regulation of $GABA_A$ receptors in nervous system pathologies. *Curr Opin Neurobiol* 22(3):552–558.
6. Ben-Ari Y, Khalilov I, Kahle KT, Cherubini E (2012) The GABA excitatory/inhibitory shift in brain maturation and neurological disorders. *Neuroscientist* 18(5):467–486.
7. Bonin RP, Orser BA (2008) $GABA_(A)$ receptor subtypes underlying general anesthesia. *Pharmacol Biochem Behav* 90(1):105–112.
8. Sine SM, Engel AG (2006) Recent advances in Cys-loop receptor structure and function. *Nature* 440(7083):448–455.
9. D'Hulst C, Atack JR, Kooy RF (2009) The complexity of the $GABA_A$ receptor shapes unique pharmacological profiles. *Drug Discov Today* 14(17-18):866–875.
10. Olsen RW, Sieghart W (2009) $GABA_A$ receptors: Subtypes provide diversity of function and pharmacology. *Neuropharmacology* 56(1):141–148.
11. Sigel E, Steinmann ME (2012) Structure, function, and modulation of $GABA_(A)$ receptors. *J Biol Chem* 287(48):40224–40231.
12. Miller PS, Aricescu AR (2014) Crystal structure of a human GABA receptor. *Nature* 512(7514):270–275.
13. Johnston GA (2014) Muscimol as an ionotropic GABA receptor agonist. *Neurochem Res* 39(10):1942–1947.
14. Amin J, Weiss DS (1993) $GABA_A$ receptor needs two homologous domains of the beta-subunit for activation by GABA but not by pentobarbital. *Nature* 366(6455):565–569.
15. Baumann SW, Baur R, Sigel E (2003) Individual properties of the two functional agonist sites in $GABA_(A)$ receptors. *J Neurosci* 23(35):11158–11166.
16. Morlock EV, Czajkowski C (2011) Different residues in the $GABA_A$ receptor benzodiazepine binding pocket mediate benzodiazepine efficacy and binding. *Mol Pharmacol* 80(1):14–22.
17. Pritchett DB, et al. (1989) Importance of a novel $GABA_A$ receptor subunit for benzodiazepine pharmacology. *Nature* 338(6216):582–585.
18. Olsen RW, Li GD (2011) $GABA(_A)$ receptors as molecular targets of general anesthetics: Identification of binding sites provides clues to allosteric modulation. *Can J Anaesth* 58(2):206–215.
19. Gurley D, Amin J, Ross PC, Weiss DS, White G (1995) Point mutations in the M2 region of the alpha, beta, or gamma subunit of the $GABA_A$ channel that abolish block by picrotoxin. *Receptors Channels* 3(1):13–20.
20. Changeux JP, Kasai M, Lee CY (1970) Use of a snake venom toxin to characterize the cholinergic receptor protein. *Proc Natl Acad Sci USA* 67(3):1241–1247.
21. Olivera BM, Quik M, Vincler M, McIntosh JM (2008) Subtype-selective conopeptides targeted to nicotinic receptors: Concerted discovery and biomedical applications. *Channels (Austin)* 2(2):143–152.
22. Rosso JP, Vargas-Rosso O, Gutiérrez JM, Rochat H, Bougis PE (1996) Characterization of alpha-neurotoxin and phospholipase A2 activities from Micrurus venoms. Determination of the amino acid sequence and receptor-binding ability of the major alpha-neurotoxin from Micrurus nigrocinctus nigrocinctus. *Eur J Biochem* 238(1): 231–239.
23. Adermann K, et al. (1999) Structural and phylogenetic characterization of human SLURP-1, the first secreted mammalian member of the Ly-6/uPAR protein superfamily. *Protein Sci* 8(4):810–819.
24. Levitin F, et al. (2008) PATE gene clusters code for multiple, secreted TFP/Ly-6/uPAR proteins that are expressed in reproductive and neuron-rich tissues and possess neuromodulatory activity. *J Biol Chem* 283(24):16928–16939.
25. Miwa JM, et al. (1999) lynx1, an endogenous toxin-like modulator of nicotinic acetylcholine receptors in the mammalian CNS. *Neuron* 23(1):105–114.
26. Sieghart W, Ramerstorfer J, Sarto-Jackson I, Varagic Z, Ernst M (2012) A novel GABA(A) receptor pharmacology: Drugs interacting with the $\alpha(+)$ $\beta(-)$ interface. *Br J Pharmacol* 166(2):476–485.
27. Eswar N, et al. (2006) Comparative protein structure modeling using Modeller. *Curr Protoc Bioinformatics* Chapter 5:Unit 5.6.

28. Nirthanan S, Gopalakrishnakone P, Gwee MC, Khoo HE, Kini RM (2003) Non-conventional toxins from Elapid venoms. *Toxicon* 41(4):397–407.
29. Antil S, Servent D, Ménez A (1999) Variability among the sites by which curaremimetic toxins bind to torpedo acetylcholine receptor, as revealed by identification of the functional residues of alpha-cobratoxin. *J Biol Chem* 274(49):34851–34858.
30. Bourne Y, Talley TT, Hansen SB, Taylor P, Marchot P (2005) Crystal structure of a Cbtx-AChBP complex reveals essential interactions between snake alpha-neurotoxins and nicotinic receptors. *EMBO J* 24(8):1512–1522.
31. Barber CM, Isbister GK, Hodgson WC (2013) Alpha neurotoxins. *Toxicon* 66:47–58.
32. Schuske K, Beg AA, Jorgensen EM (2004) The GABA nervous system in C. elegans. *Trends Neurosci* 27(7):407–414.
33. Bamber BA, Beg AA, Twyman RE, Jorgensen EM (1999) The Caenorhabditis elegans unc-49 locus encodes multiple subunits of a heteromultimeric GABA receptor. *J Neurosci* 19(13):5348–5359.
34. Jones AK, Sattelle DB (2008) The cys-loop ligand-gated ion channel gene superfamily of the nematode, Caenorhabditis elegans. *Invert Neurosci* 8(1):41–47.
35. Gregoire J, Rochat H (1977) Amino acid sequences of neurotoxins I and III of the elapidae snake Naja mossambica massambica. *Eur J Biochem* 80(1):283–293.
36. Mebs D, Narita K, Iwanaga S, Samejima Y, Lee CY (1971) Amino acid sequence of -bungarotoxin from the venom of Bungarus multicinctus. *Biochem Biophys Res Commun* 44(3):711–716.
37. Gray WR, Rivier JE, Galyean R, Cruz LJ, Olivera BM (1983) Conotoxin MI. Disulfide bonding and conformational states. *J Biol Chem* 258(20):12247–12251.
38. Johnson DS, Martinez J, Elgoyhen AB, Heinemann SF, McIntosh JM (1995) alpha-Conotoxin ImI exhibits subtype-specific nicotinic acetylcholine receptor blockade: Preferential inhibition of homomeric alpha 7 and alpha 9 receptors. *Mol Pharmacol* 48(2):194–199.
39. Marty A, Neild T, Ascher P (1976) Voltage sensitivity of acetylcholine currents in Aplysia neurones in the presence of curare. *Nature* 261(5560):501–503.
40. le Du MH, Marchot P, Bougis PE, Fontecilla-Camps JC (1989) Crystals of fasciculin 2 from green mamba snake venom. Preparation and preliminary x-ray analysis. *J Biol Chem* 264(35):21401–21402.
41. Bougis P, Rochat H, Piéroni G, Verger R (1981) Penetration of phospholipid monolayers by cardiotoxins. *Biochemistry* 20(17):4915–4920.
42. Corringer PJ, et al. (2012) Structure and pharmacology of pentameric receptor channels: From bacteria to brain. *Structure* 20(6):941–956.
43. Changeux JP (2013) The concept of allosteric modulation: An overview. *Drug Discov Today Technol* 10(2):e223–e228.
44. Christopoulos A, et al. (2014) International union of basic and clinical pharmacology. XC. multisite pharmacology: Recommendations for the nomenclature of receptor allosterism and allosteric ligands. *Pharmacol Rev* 66(4):918–947.
45. Frere RC, Macdonald RL, Young AB (1982) GABA binding and bicuculline in spinal cord and cortical membranes from adult rat and from mouse neurons in cell culture. *Brain Res* 244(1):145–153.
46. Jordan CC, Matus AI, Piotrowski W, Wilkinson D (1982) Binding of [^{3}H]gamma-aminobutyric acid and [^{3}H]muscimol in purified rat brain synaptic plasma membranes and the effects of bicuculline. *J Neurochem* 39(1):52–58.
47. Christopoulos A, Kenakin T (2002) G protein-coupled receptor allosterism and complexing. *Pharmacol Rev* 54(2):323–374.
48. Möhler H (2006) GABA($_A$) receptor diversity and pharmacology. *Cell Tissue Res* 326(2): 505–516.
49. Jones MV, Westbrook GL (1996) The impact of receptor desensitization on fast synaptic transmission. *Trends Neurosci* 19(3):96–101.
50. Brickley SG, Mody I (2012) Extrasynaptic GABA($_A$) receptors: Their function in the CNS and implications for disease. *Neuron* 73(1):23–34.
51. Chang Y, Ghansah E, Chen Y, Ye J, Weiss DS (2002) Desensitization mechanism of GABA receptors revealed by single oocyte binding and receptor function. *J Neurosci* 22(18):7982–7990.
52. Tia S, Wang JF, Kotchabhakdi N, Vicini S (1996) Distinct deactivation and desensitization kinetics of recombinant GABA$_A$ receptors. *Neuropharmacology* 35(9-10): 1375–1382.
53. Weber M, Changeux JP (1974) Binding of Naja nigricollis (^{3}H)alpha-toxin to membrane fragments from Electrophorus and Torpedo electric organs. I. Binding of the tritiated alpha-neurotoxin in the absence of effector. *Mol Pharmacol* 10(1):1–14.
54. Olsen RW, Sieghart W (2008) International Union of Pharmacology. LXX. Subtypes of gamma-aminobutyric acid(A) receptors: Classification on the basis of subunit composition, pharmacology, and function. Update. *Pharmacol Rev* 60(3):243–260.
55. Bianchi MT, Botzolakis EJ, Lagrange AH, Macdonald RL (2009) Benzodiazepine modulation of GABA($_A$) receptor opening frequency depends on activation context: A patch clamp and simulation study. *Epilepsy Res* 85(2-3):212–220.
56. Mortensen M, Smart TG (2006) Extrasynaptic alphabeta subunit GABA$_A$ receptors on rat hippocampal pyramidal neurons. *J Physiol* 577(Pt 3):841–856.
57. Albuquerque EX, Pereira EF, Alkondon M, Rogers SW (2009) Mammalian nicotinic acetylcholine receptors: From structure to function. *Physiol Rev* 89(1):73–120.
58. Zouridakis M, Zisimopoulou P, Poulas K, Tzartos SJ (2009) Recent advances in understanding the structure of nicotinic acetylcholine receptors. *IUBMB Life* 61(4): 407–423.
59. Ganguly K, Schinder AF, Wong ST, Poo M (2001) GABA itself promotes the developmental switch of neuronal GABAergic responses from excitation to inhibition. *Cell* 105(4):521–532.
60. Dutertre S, Lewis RJ (2010) Use of venom peptides to probe ion channel structure and function. *J Biol Chem* 285(18):13315–13320.
61. Platt RJ, et al. (2014) From molecular phylogeny towards differentiating pharmacology for NMDA receptor subtypes. *Toxicon* 81:67–79.
62. Kalia J, et al. (2015) From Foe to Friend: Using Animal Toxins to Investigate Ion Channel Function. *J Mol Biol* 427(1):158–175.
63. Ye JH, McArdle JJ (1997) Waglerin-1 modulates gamma-aminobutyric acid activated current of murine hypothalamic neurons. *J Pharmacol Exp Ther* 282(1):74–80.
64. McCann CM, Bracamontes J, Steinbach JH, Sanes JR (2006) The cholinergic antagonist alpha-bungarotoxin also binds and blocks a subset of GABA receptors. *Proc Natl Acad Sci USA* 103(13):5149–5154.
65. Savage JM (2002) *The amphibians and reptiles of Costa Rica: A herpetofauna between two continents, between two seas* (The University of Chicago Press, Chicago).
66. Thompson SA, Whiting PJ, Wafford KA (1996) Barbiturate interactions at the human GABA$_A$ receptor: Dependence on receptor subunit combination. *Br J Pharmacol* 117(3):521–527.
67. Farrant M, Nusser Z (2005) Variations on an inhibitory theme: Phasic and tonic activation of GABA($_A$) receptors. *Nat Rev Neurosci* 6(3):215–229.
68. Köhling R (2002) Neuroscience. GABA becomes exciting. *Science* 298(5597): 1350–1351.
69. Chavas J, Marty A (2003) Coexistence of excitatory and inhibitory GABA synapses in the cerebellar interneuron network. *J Neurosci* 23(6):2019–2031.
70. Gordon D, et al. (1996) Scorpion toxins affecting sodium current inactivation bind to distinct homologous receptor sites on rat brain and insect sodium channels. *J Biol Chem* 271(14):8034–8045.
71. Rey-Suárez P, Núñez V, Gutiérrez JM, Lomonte B (2011) Proteomic and biological characterization of the venom of the redtail coral snake, Micrurus mipartitus (Elapidae), from Colombia and Costa Rica. *J Proteomics* 75(2):655–667.
72. Retief JD (2000) Phylogenetic analysis using PHYLIP. *Methods Mol Biol* 132:243–258.
73. Löwenadler B, et al. (1987) A gene fusion system for generating antibodies against short peptides. *Gene* 58(1):87–97.
74. Drevet P, et al. (1997) High-level production and isotope labeling of snake neurotoxins, disulfide-rich proteins. *Protein Expr Purif* 10(3):293–300.
75. Pieper U, et al. (2011) ModBase, a database of annotated comparative protein structure models, and associated resources. *Nucleic Acids Res* 39(Database issue): D465–D474.
76. Pettersen EF, et al. (2004) UCSF Chimera—a visualization system for exploratory research and analysis. *J Comput Chem* 25(13):1605–1612.
77. Marchot P, Khélif A, Ji YH, Mansuelle P, Bougis PE (1993) Binding of 125I-fasciculin to rat brain acetylcholinesterase. The complex still binds diisopropyl fluorophosphate. *J Biol Chem* 268(17):12458–12467.
78. Gray EG, Whittaker VP (1962) The isolation of nerve endings from brain: An electron-microscopic study of cell fragments derived by homogenization and centrifugation. *J Anat* 96:79–88.
79. Maas C, et al. (2006) Neuronal cotransport of glycine receptor and the scaffold protein gephyrin. *J Cell Biol* 172(3):441–451.
80. Accardi MV, et al. (2014) Mitochondrial reactive oxygen species regulate the strength of inhibitory GABA-mediated synaptic transmission. *Nat Commun* 5:3168.